A PHYSICAL MODELLING OF A DC PLASMA TORCH

J.M. Bauchire, J.J. Gonzalez, A. Gleizes

CPAT - URA du C.N.R.S. n°277- Université Paul Sabatier
118 route de Narbonne- F31062 Toulouse cedex- France

ABSTRACT

A mathematical representation is developed describing the temperature and the velocity profiles in an argon plasma jet discharging into argon. We present the influence of the mass flow rate and of the arc current on the characteristics of the plasma. The comparison of turbulence models with the laminar flow shows the importance of their consideration and also the critical role of the boundary conditions.

1/ INTRODUCTION

In order to provide high-quality for specialized applications or to help the development of the technology, many studies of electric arcs, especially non transferred arcs are made. The comparison between experimental results and the modelling leads to refine the calculation by taking into account more and more sophisticated phenomena. The majority of these works are made in an argon plasma discharging into argon. We can hold for example the measurements of Capetti and E. Pfender [1] and Dilawari et al [2]. Others works of McKelliget et al [3] or Chang and Ramshaw [4] have treated numerical simulations of argon plasma jets flowing respectively into cold air and nitrogen. For all these applications the behaviour of the plasma is essential, through the study of the turbulence. We cannot forget to mention the paper of Huang et al [5] about a two-fluid model of turbulence which can predict phenomena that escape to the more conventional model, e.g. the unmixing calculations. In the mentioned studies the modelling of the free plasma jet requires the adjustable data of the temperature and of the axial velocity profiles. Seungho Paik et al [6] have studied the determination of the arc-root position in a DC plasma torch, but this model is not coupled with the interactions on the free plasma jet. This paper is a preliminary study of the modelling of a plasma torch in the nozzle and in the free jet regions. With an arbitrary configuration we have studied the influence of geometrical parameters on the velocities and on the temperature profiles. Our results show the importance of turbulence treated by three models compared with a laminar flow and the critical role of the boundary conditions.

2/ MODELLING

2.1/ Assumptions and governing equations

The model adopted is based on the following assumptions:

The governing equations are written in an axisymetric system of coordinates and the operation of the torch is assumed to be in a steady state with negligible gravity effects. The plasma is assumed to be optically thin and in local thermodynamic equilibrium (LTE).

Based on these assumptions, solutions are sought for a set of elliptical partial differential transport equations that all have the same form:

$$\frac{\partial}{\partial x}(\rho u\phi) + \frac{1}{r}\frac{\partial}{\partial r}(r\rho v\phi) = \frac{\partial}{\partial x}\left(\Gamma_\phi \frac{\partial \phi}{\partial x}\right) + \frac{1}{r}\frac{\partial}{\partial r}\left(r\Gamma_\phi \frac{\partial \phi}{\partial r}\right) + S_\phi \qquad (1)$$

where ϕ is the general variable, Γ_ϕ the corresponding diffusion coefficient and S_ϕ the source term. u and v are the axial and radial velocity components, ρ is the mass density, x and r are the distances in the axial and radial directions respectively. The terms of the governing equations are represented below.

Table 1 : Terms of the governing equations

Conservation of	ϕ	Γ_ϕ	S_ϕ
Mass	1	0	0
Axial momentum	u	μ_e	$\frac{\partial}{\partial x}\left(\mu_e \frac{\partial u}{\partial x}\right) + \frac{1}{r}\frac{\partial}{\partial r}\left(r\mu_e \frac{\partial v}{\partial r}\right) - \frac{\partial p}{\partial x} + j_r B_\theta$
Radial momentum	v	μ_e	$\frac{\partial}{\partial x}\left(\mu_e \frac{\partial u}{\partial r}\right) + \frac{1}{r}\frac{\partial}{\partial r}\left(r\mu_e \frac{\partial v}{\partial x}\right) - 2\mu_e \frac{v}{r^2} - \frac{\partial p}{\partial x} - j_x B_\theta$
Energy	h	$\frac{K}{C_p} + \frac{\mu_t}{Pr_T}$	$\frac{j^2_x + j^2_r}{\sigma} - 4\pi\varepsilon_N + \frac{5}{2}\frac{k_B}{e}\left(\frac{j_x}{C_p}\frac{\partial h}{\partial x} + \frac{j_r}{C_p}\frac{\partial h}{\partial r}\right)$
Turbulent kinetic energy	k	$\mu + \frac{\mu_t}{Pr_k}$	$G - \rho\varepsilon$
Turbulent dissipation rate	ε	$\mu + \frac{\mu_t}{Pr_\varepsilon}$	$C_{\varepsilon 1} G \frac{\varepsilon}{k} - \rho C_{\varepsilon 2} \frac{\varepsilon^2}{k}$

where p is the local pressure, h the specific enthalpy, k the turbulent kinetic energy and ε the turbulent dissipation rate. μ_e, μ, μ_t, C_p, K and σ are the effective, laminar and turbulent viscosities, the specific heat, and thermal and electrical conductivities. k_B is the Boltzmann's constant, e is the elementary charge of the electron, j_r and j_x are the radial and axial current density components, B_θ is the azimuthal component of the magnetic field and ε_N the net emission coefficient of the plasma.

2.2/ Turbulence models

The turbulence nature of the flow is represented through the effective viscosity which is the sum of the molecular and the turbulent viscosities.

2.2.1/ The zero-equation model

This model is based on the Prandtl's mixing length hypothesis: $\mu_t = \rho l_m^2 \left|\frac{\partial u}{\partial x}\right|$. Based on Nicolet's work [7], we have adopted the following expressions of the mixing length l_m and Prandtl's number Pr_T:

for $y \le y_c$, $$l_m = 0.4y\left[1 - \exp\left(\frac{-y\sqrt{\rho\mu^* \left|\frac{\partial u}{\partial r}\right|^*}}{26\mu^*}\right)\right] \quad (2)$$

for $y_c \le y \le R$, $$l_m = 0.075\ R \quad (3)$$

for $y \ge 0.05\ R$, $$Pr_T = 0.95 - 0.45\left(\frac{y}{R}\right)^2 \quad (4)$$

for $y < 0.05\ R$, $$Pr_T = 3 - \frac{20y}{R}(3 - 0.949) \quad (5)$$

where R is the pipe radius, y is the distance from pipe wall as $y = R-r+r_g$, r_g is the wall roughness distance. y_c is obtained from the continuity of l_m and * values are taken at the wall. In the plume region, two cases are studed: case I, the mixing length and Prandtl's number expressions are taken from the work of Gonzalez [8], that is equation (3) for the mixing length, equation (4) if $r < R$ and $Pr_T = 0.95$ if $r \ge R$. Case II, a standard expression of mixing length for free jet is used [9] : $\begin{cases} l_m = C(r_1 - r_2) \\ Pr_T = 0.7 \end{cases}$

r_1 and r_2 are two radial positions chosen such that the velocity is equal to 0.2 and 0.8 times the centerline velocity for r_1 and r_2. C is a constant that can be determinated by experimental studies. Here C is equal to 0.8 in order to be in agreement with case I.

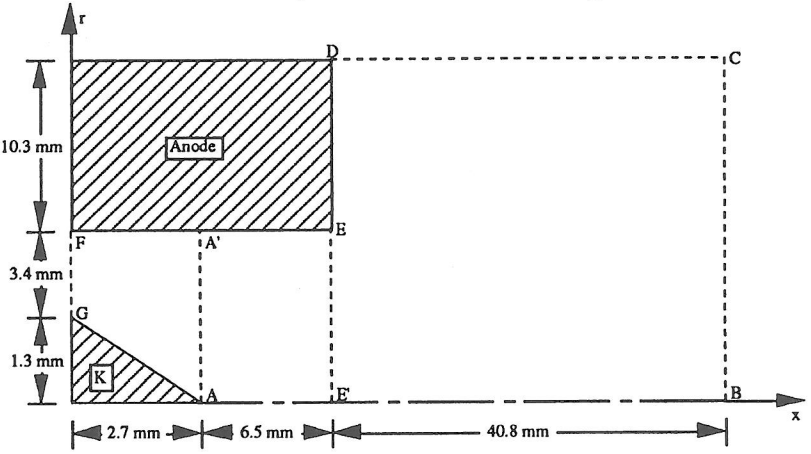

Fig. 1 : Computation domain

2.2.2/ The two-equation model

The turbulent viscosity can be obtained by a k-ε model [10-13],with $\mu_t = C_\mu \rho \frac{k^2}{\varepsilon}$.

Table 2 : Constant values

$C_{\varepsilon 1}$	$C_{\varepsilon 2}$	C_μ	Pr_T	Pr_k	Pr_ε
1.44	1.92	0.09	0.7	1.0	1.3

The turbulent kinetic energy and the dissipation rate are calculated via the transport

equation shown in Table 1 with $G = 2\mu_t\left\{\left(\frac{\partial u}{\partial x}\right)^2+\left(\frac{\partial v}{\partial r}\right)^2+\left(\frac{v}{r}\right)^2+\frac{1}{2}\left(\frac{\partial u}{\partial r}+\frac{\partial v}{\partial x}\right)^2\right\}$. Values of constants are given in Table 2 with modifications for free jets [14]:

$$\begin{cases} C_\mu = 0.09 - 0.04\ f \\ C_2 = 1.92 - 0.0667\ f \\ f = \left|\frac{\delta}{2\Delta u}\left(\frac{\partial u_o}{\partial x} - \left|\frac{\partial u_o}{\partial x}\right|\right)\right|^{0.2} \end{cases}$$

where δ is the boundary layer thickness, Δu is the velocity difference between centerline and free stream velocities and u_o is the centerline velocity.

2.3/ Calculation domain and boundary conditions

The calculation region is sketched in Fig. 1 and the corresponding boundary conditions are given in Table 3. The potential is set to zero on the line EE' and axisymmetric conditions are set on the center line. The current density in the cathode spot, on line AA', is represented by an exponential function after Hsu and co-workers [15].The plasma properties of the argon gas are function of temperature and the governing equations are solved using Patankar's algorithms [16].

Table 3 : Boundary conditions

	AB	BC	CD	DF	FG	GA
u	$\frac{\partial u}{\partial r}=0$	$\frac{\partial u}{\partial x}=0$	$u=0$	$u=0$	$u=u(r)$	$u=0$
v	$v=0$	$\frac{\partial v}{\partial x}=0$	$\frac{\partial v}{\partial r}=0$	$v=0$	$v=0$	$v=0$
T	$\frac{\partial T}{\partial r}=0$	$\frac{\partial T}{\partial x}=0$	$T=500$ K	$T=1000$K	$T=300$ K	$T=3000$ K
k	$\frac{\partial k}{\partial r}=0$	$\frac{\partial k}{\partial x}=0$	$\frac{\partial k}{\partial r}=0$	$k=0$	$k=0$	$k=0$
ε	$\frac{\partial \varepsilon}{\partial r}=0$	$\frac{\partial \varepsilon}{\partial x}=0$	$\frac{\partial \varepsilon}{\partial r}=0$	$\varepsilon=0$	$\varepsilon=0$	$\varepsilon=0$

3/ RESULTS

We have made a study on geometrical and physical parameters. The influence of the radial and axial dimensions of the computational domain has been studied. For this comparison mesh grids 35x85 (5 cm) and 35x167 (10 cm) have been used for the study of the axial distance and grids 35x85 (1.5 cm) and 42x85 (3 cm) for the effect of the radius. The good agreement between the values leads us to use the 35x85 grid.

One of the initial conditions is the inlet velocity profile. Three initial profiles were used : a parabolic, a constant and a Couette's profile. It can be noted that the difference between the three profiles diminishes when the power of the arc becomes greater. In all the cases the maximum difference on the velocity on the free plasma jet is about 5%. The range of the operating parameters is 50A<I<400A for the intensity and 0.1g/s<D<1.2g/s for the mass flow rate. We present now the influence of the arc intensity and the mass flow rate on the temperature and velocity profiles in the nozzle and in the free plasma jet considering laminar and turbulent flows (cf: §2).

For two current intensities 100A and 200A and the turbulent model I, we have

plotted the evolution of the mass flow rate. In the laminar flow (figure 2) an increase of the current intensity leads to a rise of the mass flow rate by the pumping of the surrounding gas. The evolution of the mass flow rate is an agreement with the works of Pateyron [17]. For an axial distance equal to four times the diameter, the mass flow rate D has a value about three times the initial value. The use of turbulent model I shows an increase of the surrounding gas pumping, the evolution remains on Pateyron's predictions. In our study, we have not taken systematically into account the work of Paik et al [6] about the arc root position in the torch. These authors show that the arc is longer when the mass flow rate or the diameter increases. However a diminution of the arc intensity which leads to an increase of the arc length. In the figure 3 a we have plotted, for a mass flow rate equal to 0.5 g/s, the isotherms of the plasma respectively for an arc intensity equal to 100A and a zero potential at the exit of the nozzle (X_1 from the anode) and 200A and a zero potential position at $X_2=0.5X_1$, to be compared with figure 3-b. We obtained the same conclusion on the behaviour of the plasma with a difference of about 3000K taking into account Paik's works.

Using turbulence models described in section 2, we can see on figures 4-5 a critical decrease of axial velocity and axial temperature profiles beetwen laminar and turbulent fluid flows due to an increase of viscosity and entrainment of cold gas. The comparison of the two mixing length models shows a good agreement on the two profiles. We have obtained the same results with a current intensity of 200 A and a mass flow rate of 1 g/s. The k-ε model leads to higher values on velocity and temperature profiles. The difference seems to appear during the nozzle portion and remains the same along the free jet. Yet the standard k-ε model is not applicable near the wall so we will have to take into account the influence of the pipe wall like Murphy [13] by a wall-function method or a low-Reynolds-number method [10]. On the other hand, we noted the important role of the boundary conditions of k and ε discussed by McKelliget [3]. In conclusion, though the turbulence model (case II) seems to be the most computationally, refinement of the model had to be undertaken in conjunction with experimental studies especially for the determination of the constant values.

REFERENCES

[1] A. Capetti and E. Pfender, Plasma Chem. and Plasma Proc., 9, 329 (1989)
[2] A.H. Dilawari et al, Plasma Chem. and Plasma Proc., 10, 321 (1990)
[3] J. McKelliget et al, Plasma Chem. and Plasma Proc., 2, 31 (1982)
[4] C.H. Chang and J.D. Ramshaw, Plasma Chem. and Plasma Proc., 13, 189 (1993)
[5] P.C. Huang et al, Plasma Chem. and Plasma Proc., 15, 25 (1995)
[6] Seungho Paik et al, Plasma Chem. and Plasma Proc., 13, 379 (1993)
[7] W.E. Nicolet et al, Acurex Corporation, AEDC.TR.75.47
[8] J.J. Gonzalez, Thèse de l'Université Paul Sabatier, n° 1100 (1992)
[9] P. Proulx, Thèse de Doctorat, Université de Sherbrooke (1987)
[10] B.E. Launder and D.B. Spalding, Comp.Meth. Appl. Mech. Eng., 3, 269 (1974)
[11] Y.P. Chyou and E. Pfender, Plasma Chem. and Plasma Proc., 9, 291 (1989)
[12] D.A. Scott et al, J. Appl. Phys., 66, 5232 (1989)
[13] A.B. Murphy and P. Kovitya, J. Appl. Phys., 73, 4759 (1993)
[14] W. Rodi, Ph. D. Thesis, University of London (1972)
[15] K.C. Hsu, K. Etemadi and E. Pfender, J. Appl. Phys., 54, 3, 1293 (1983)
[16] S.V. Patankar, *Numerical Heat Transfer and Fluid Flow*, McGraw-Hill (1980)
[17] B. Pateyron, Thèse de Doctorat ès-sciences, n° 21-1987, Limoges (1987)

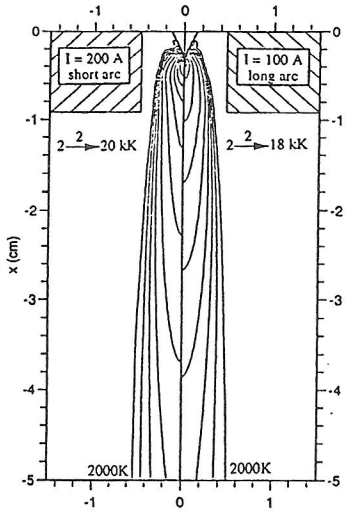

Fig. 3-a : Influence of the length of the arc

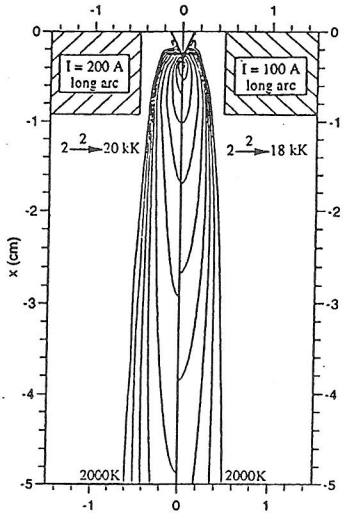

Fig. 3-b : Influence of the intensity of the arc

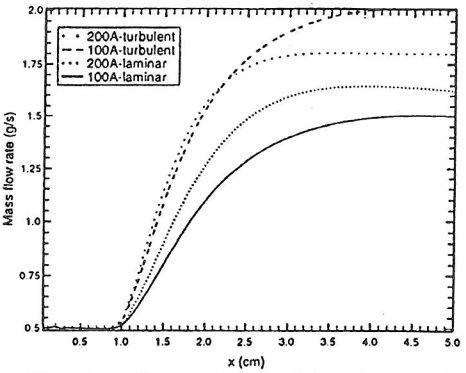

Fig. 2 : Comparison of laminar and turbulent flows

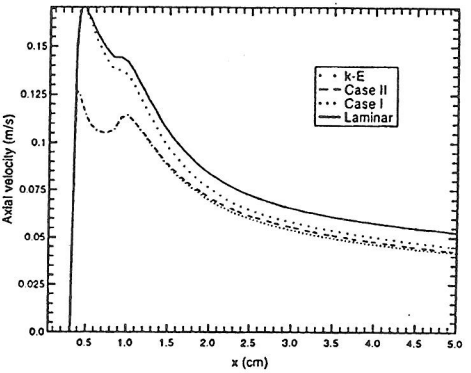

Fig. 4 : Axial velocity profile on center line (I=100A, D_0=5g/s)

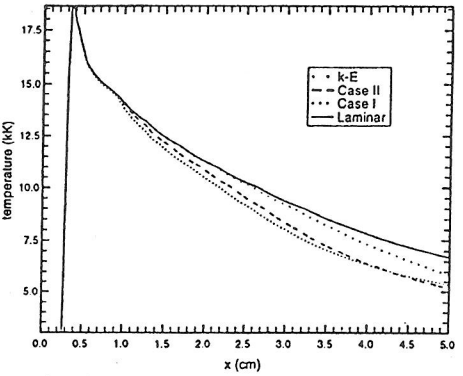

Fig. 5 : Temperature profile on center line (I=100A, D_0=5g/s)